Photosynthesis Research (2021) 147:229–237
https://doi.org/10.1007/s11120-020-00813-z

ORIGINAL ARTICLE

# $Ca^{2+}$ effects on Fe(II) interactions with Mn-binding sites in Mn-depleted oxygen-evolving complexes of photosystem II and on Fe replacement of Mn in Mn-containing, Ca-depleted complexes

**B. K. Semin[1] · L. N. Davletshina[1] · S. N. Goryachev[1] · M. Seibert[2]**

Received: 17 August 2020 / Accepted: 11 December 2020 / Published online: 2 February 2021


## Abstract

Fe(II) cations bind with high efficiency and specificity at the high-affinity (HA), Mn-binding site (termed the "blocking effect" since Fe blocks further electron donation to the site) of the oxygen-evolving complex (OEC) in Mn-depleted, photosystem II (PSII) membrane fragments (Semin et al. in Biochemistry 41:5854, 2002). Furthermore, Fe(II) cations can substitute for 1 or 2Mn cations (pH dependent) in Ca-depleted PSII membranes (Semin et al. in Journal of Bioenergetics and Biomembranes 48:227, 2016; Semin et al. in Journal of Photochemistry and Photobiology B 178:192, 2018). In the current study, we examined the effect of $Ca^{2+}$ cations on the interaction of Fe(II) ions with Mn-depleted [PSII(-Mn)] and Ca-depleted [PSII(-Ca)] photosystem II membranes. We found that $Ca^{2+}$ cations (about 50 mM) inhibit the light-dependent oxidation of Fe(II) (5 μM) by about 25% in PSII(-Mn) membranes, whereas inhibition of the blocking process is greater at about 40%. Blocking of the HA site by Fe cations also decreases the rate of charge recombination between $Q_A^-$ and $Y_Z^{\bullet+}$ from $t_{1/2} = 30$ ms to 46 ms. However, $Ca^{2+}$ does not affect the rate during the blocking process. An Fe(II) cation (20 μM) replaces 1Mn cation in the $Mn_4CaO_5$ catalytic cluster of PSII(-Ca) membranes at pH 5.7 but 2 Mn cations at pH 6.5. In the presence of $Ca^{2+}$ (10 mM) during the substitution process, Fe(II) is not able to extract Mn at pH 5.7 and extracts only 1Mn at pH 6.5 (instead of two without $Ca^{2+}$). Measurements of fluorescence induction kinetics support these observations. Inhibition of Mn substitution with Fe(II) cations in the OEC only occurs with $Ca^{2+}$ and $Sr^{2+}$ cations, which are also able to restore oxygen evolution in PSII(-Ca) samples. Nonactive cations like $La^{3+}$, $Ni^{2+}$, $Cd^{2+}$, and $Mg^{2+}$ have no influence on the replacement of Mn with Fe. These results show that the location and/or ligand composition of one Mn cation in the $Mn_4CaO_5$ cluster is strongly affected by calcium depletion or rebinding and that bound calcium affects the redox potential of the extractable Mn4 cation in the OEC, making it resistant to reduction.

**Keywords** Photosystem II · Oxygen-evolving complex · Iron · Manganese · Manganese replacement · Calcium

## Abbreviations

| | |
|---|---|
| Chl | Chlorophyll |
| DCMU | 3-(3,4-Dichlorophenyl)-1,1-dimethylurea |
| DCPIP | 2,6-Dichlorophenolindophenol |
| HA | High-affinity Mn-binding site [also known as the site where the "dangler" cation (Mn #4 of the Suga et al. 2015 structure) binds] |
| $F_0$ | Fluorescence emitted by a sample at low light levels prior to flash excitation |
| $(F - F_0)/F_0$ | Fluorescence yield |
| $F_{max}$ | Maximum fluorescence yield following actinic flash excitation |
| $F_{fin}$ | Final fluorescence yield detected after decay of the flash-induced fluorescence |
| MES | 2-(*N*-Morpholino)-ethanesulfonic acid |
| OEC | Oxygen-evolving complex |
| PSII | Photosystem II |

✉ B. K. Semin
semin@biophys.msu.ru

[1] Department of Biophysics, Faculty of Biology, Lomonosov Moscow State University, Moscow, Russia 119234

[2] Laboratory, BioEnergy Sciences and Technology Directorate, National Renewable Energy, Golden, CO 80401, USA

| | |
|---|---|
| PSII(-Ca) | $Ca^{2+}$-depleted PSII membranes with 4 Mn cations in the OEC |
| PSII(-Mn) | Mn-depleted PSII membranes |
| PSII(-Mn,+Fe) | PSII(-Mn) membranes blocked by an iron cation at the high-affinity Mn-binding site |
| RC | Reaction center |
| TMB | 3,3′,5,5′-Tetramethylbenzidine |
| Tris | Tris(hydroxymethyl)aminomethane |

## Introduction

Oxygen in the atmosphere is generated during the light-dependent oxidation of water, which is catalyzed by the photosynthetic $O_2$-evolving complex (OEC) of photosystem II (PSII) in plants, algae, and cyanobacteria. The catalytic center of the OEC is the inorganic cluster, $Mn_4CaO_5$ (Umena et al. 2011). It synthetizes the molecular bond linking the oxygen atoms of two water molecules and operates continuously by cycling through five redox states (the 'Kok cycle'). During this cycle, the OEC extracts water protons and electrons that are used to drive ATP and NADPH formation. Molecular oxygen is released into biosphere as the byproduct of the cycle. Understanding of the $Mn_4CaO_5$ catalyst structure has rapidly advanced over the past few years due to novel X-ray crystallography technology. Umena et al. (Umena et al. 2011) performed X-ray diffraction analysis at a resolution of 1.9 Å on PSII core preparations from *Thermosynechococcus vulcanus* (a thermophilic cyanobacterium) in the dark-stable S1-state. Such high resolution allowed them to determine the structure of the cluster, to reveal four molecules of water (W1–W4) within the cluster (they provide ligands to Mn4 and Ca) and to identify a number of polypeptide ligands to Mn4 and Ca. The $Mn_4CaO_5$ cluster is a distorted cube formed by 3Mn cations and 1Ca cation connected by oxygen bridges, and the 4th Mn cation is bound to the cluster by two oxygen bridges labeled O4 and O5. Recently, a "radiation-damage-free" structure of PSII, which eliminates the X-ray-induced reduction of the Mn cations during the measurements, was determined using X-ray pulses of femtosecond duration (Suga et al. 2015). Furthermore, the OEC structure of in higher S states than the dark-stable S1-state has also been investigated using an X-ray laser source at room temperature (Suga et al. 2017; Kern et al. 2018). Nevertheless, the exact mechanism of the PSII water-splitting reaction remains unclear despite the availability of an atomic structure of the OEC.

Due to similarities between the redox and atomic properties of manganese and iron cations, Fe(II) cations under oxidizing conditions can bind to unoccupied Mn-binding sites [as Fe(III)] with very high specificity and affinity in Mn-depleted, PSII membrane fragments [PSII(-Mn), hereafter] when they are illuminated (Semin et al. 2002; Semin and Seibert 2004, 2006). Interaction of Fe(II) cations with the donor side of the PSII(-Mn) membrane is reminiscent in fact of the Mn-photoligation steps of the photoactivation process (Tamura and Cheniae 1987; Ananyev and Dismukes 1996). An Fe(II) cation binds to the high-affinity (HA), Mn-binding site at micromolar concentrations, and the bound cation is oxidized by $Y_Z^{\bullet+}$ under weak illumination since light is a necessary factor for cation ligation (Semin et al. 2002). The resultant Fe(III) cation blocks the HA site (i.e., prevents the interaction of additional added Mn(II) cations with the site), but 4–5 Fe(II) cations must be oxidized in order to observe the blocking effect (Semin and Seibert 2004). The bound Fe(III) cation is coordinated at the HA site by a carboxylic group (Semin and Seibert 2006). All these results demonstrate the high specificity of Fe cation interactions with OEC Mn-binding sites.

In addition to the above method of Mn substitution with Fe, the binding of Fe cations at Mn-binding sites in the OEC can be accomplished using another simple method. Ca-depleted PSII (PSII[-Ca]) membranes contain the Mn cluster but lack two of the three extrinsic proteins (PsbP and PsbQ, Ghanotakis et al. 1984a) that normally cover and protect the Mn cluster from destruction. As a result, the Mn cluster is open to reduction by exogenous reductants (Ghanotakis et al. 1984b). If a Mn(II) cation is reduced, it is rapidly released from its binding site. If exogenous Fe(II) cations are the reductant, Fe(III) forms and occupies the empty Mn site, because Fe has a higher specific affinity for the HA Mn-binding site than Mn itself. Using such an approach, we found that Fe(II) cations can substitute for 2Mn cations in PSII(-Ca) membranes at pH 6.5 (Semin and Seibert 2016) and 1Mn ion at pH 5.7 (Semin et al. 2018). Another metal cation essential in the OEC for the water-splitting reaction is the redox-inactive metal, $Ca^{2+}$ (see Najafpour et al. 2016, for a review). Although its role has not been fully elucidated, there have been several recent structural and functional hypotheses. Brudvig and his co-workers proposed that $Ca^{2+}$ acts as a Lewis acid, binding a water substrate molecule and hence tuning its reactivity (Vrettos et al. 2001a). Kim and Debus (2017), using FTIR difference spectroscopy, identified water molecule, W3, bound to a Ca cation, as the substrate becoming part of the O–O bond of the $O_2$ released from the OEC during a water-splitting cycle. Recently Tsui and Agapie (2013) found a linear dependence between the heterometallic metal–oxido cluster potential and the Lewis acidity of redox-inactive metal cations. They suggested that this correlation provides evidence for the role of the $Ca^{2+}$ ion in modulating redox potential of the manganese cluster. Taking this into account, we investigated the interaction of Ca- and Mn-binding sites and the effect of $Ca^{2+}$ cations on Fe cation substitution for Mn, based on the reduction of Mn by Fe cations.

## Materials and methods

*Spinach PSII-enriched membranes* were prepared according to Ghanotakis and Babcock (1983). The rates of $O_2$ evolution (450–550 µmol $O_2$ mg chlorophyll (Chl)$^{-1}$ h$^{-1}$) were measured polarographically with 0.2 mM 2,6-dichloro-1,4-benzoquinone as the exogenous electron acceptor. Samples were stored at − 80 °C in 50 mM 2-(*N*-morpholino)-ethanesulfonic acid (MES) at pH 6.5, 15 mM NaCl, and 400 mM sucrose (buffer A). Chlorophyll concentrations were measured in 80% acetone (Porra et al. 1989).

*The photoreduction rate of the exogenous electron acceptor 2,6-dichlorophenolindophenol (DCPIP)* was determined spectrophotometrically from the change in absorbance at 600 nm, using the molar extinction coefficient for the deprotonated form of DCPIP ($\varepsilon = 21.8$ mM$^{-1}$ cm$^{-1}$ Armstrong 1964).

*Tris-HCl extraction of manganese [PSII(-Mn) samples] from the OEC.* PSII membranes (0.5 mg Chl ml$^{-1}$) were incubated in a 1 M Tris-HCl buffer (pH 9.4), containing 0.4 M sucrose, for 30 min at 4 °C under room (fluorescent) light (Preston and Seibert 1991). The pelleted membranes were washed twice with buffer A and resuspended in the same buffer. The functional manganese cluster and the three extrinsic polypeptides (17, 23, and 33 kDa) required for photosynthetic oxygen evolution were removed by this treatment (Ghirardi et al. 1996).

*Ca-depleted PSII [PSII(-Ca)] membranes* were prepared by incubating PSII membranes in buffer, containing 2 M NaCl, 0.4 M sucrose, and 25 mM MES (pH 6.5) (Ono and Inoue 1990). The preparations were incubated in the buffer for 15 min at room temperature under low illumination (4–5 µE m$^{-2}$ s$^{-1}$, room fluorescent light). The resulting material was then washed twice with buffer A. Besides, $Ca^{2+}$ PSII(-Ca) membranes lack the PsbQ and PsbP extrinsic proteins, which prevent exogenous reducing agents from attacking the Mn/Ca cluster.

*PSII samples with the HA Mn-binding site blocked by Fe cations [PSII(-Mn,+Fe)]* were obtained according to the method described in Semin et al. (2002). PSII(-Mn) membranes (25 µg Chl ml$^{-1}$) were incubated in buffer A (pH 6.5) containing 5 µM Fe(II) for 3 min under low light (5 µE m$^{-2}$ s$^{-1}$) and constant stirring. After incubation, the preparations were precipitated by centrifugation, washed, and resuspended in buffer A.

*PSII preparations with a heterogeneous 2Mn–2Fe cluster in the OEC [PSII(2Mn,2Fe)]* were obtained by the method developed by Semin and Seibert (2016). PSII(-Ca) membranes (100 µg Chl ml$^{-1}$) were incubated with ferrous sulfate (20 µM) in buffer A (pH 6.5) for 120 min at 4 °C in the dark. After incubation, the membranes were precipitated by centrifugation, washed, and resuspended in buffer A. The resulting membrane fragments contained precisely two Mn cations and two Fe(III) cations per reaction center in every center (Semin and Seibert 2016).

*Flash-probe fluorescence* (for measurement of the flash-induced Chl fluorescence decay kinetics) was monitored at 22 °C using a lab-built apparatus (Ghirardi et al. 1996). Membrane suspensions (25 µg Chl ml$^{-1}$ in buffer A) were excited with a saturating actinic, single-turnover xenon flash (3 µs) passed through a Corion LS-650 low-bandpass filter. Weak monitoring flashes were provided by an array of Hewlett-Packard light-emitting diodes. Dark-adapted samples contained 40 µM DCMU. Fluorescence emission ($F$), normalized to the fluorescence emitted by the samples due to weak monitoring flashes prior to excitation with a saturating flash (the fluorescence termed $F_0$), was represented in the figures as the ratio $(F - F_0)/F_0$ (Ghirardi et al. 1996).

*Mn concentrations in different samples* were measured as described in a previous publication (Semin and Seibert 2009). Samples (100 µg Chl) were suspended in 1 ml of buffer A and then incubated with 50 mM $CaCl_2$ for 2 min in the dark at 5 °C. After incubation, the samples were microfuged to remove any non-specifically bound Mn. The membrane pellet was resuspended in 90 µl of 0.6 N HCl (pellet volume, about 10 µl) to solubilize the functional Mn remaining in the pellet. Next, 0.9 ml of deionized/glass-distilled water was added to the membrane suspension, and finally, the microfuge tube was centrifuged for 3 min at 15,000×*g* (22 °C). The supernatant (0.9 ml) was filtered through a 13-mm Acrodisc syringe filter containing a 0.2 µm nylon membrane (Pall Life Sciences, Ann Arbor, USA). The filtrate (in a 1-ml glass/quartz cuvette) was mixed consecutively according to Serrat (1998) with 40 µl of 2 M NaOH, 40 µl of a stock solution of 3,3′,5,5′-tetramethylbenzidine (TMB) (100 mg TMB in 100 ml of 0.1 M hydrochloric acid), and 40 µl of 5.3 M phosphoric acid. The absorbance at 450 nm was used to calculate Mn(II) concentrations (extinction coefficient of 34 mM$^{-1}$ cm$^{-1}$) in the samples (Serrat 1998). PSII reaction center (RC) concentrations were calculated in µM using 250 molecules of Chl/RC in the PSII samples (Ghanotakis et al. 1984c; Xu and Bricker 1992).

*Fluorescence induction kinetics (FIK)* were measured under constant saturating (1200 µE m$^{-2}$ s$^{-1}$) light using a Hansatech Instruments, Ltd. (England), Plant Efficiency Analyzer. LEDs (with $\lambda_{max}$ at 650 nm and a spectral range of 580–710 nm) were used as the source of excitation light. The fluorescence signal, measured 50 µs after switching on the steady light source, was used as the $F_0$ value. The sample was illuminated for 2 s. A common logarithmic scale was used to construct the FIK graphs.

## Results and Discussion

### $Ca^{2+}$ effects on the interaction of Fe(II) cations with the HA Mn-binding site in the OEC

The HA Mn-binding site contains a carboxylic group ligand (amino acid residue, D1–D170 Nixon and Diner 1992). According to X-ray diffraction analysis (Umena et al. 2011), the HA site in intact membranes is occupied by a Mn cation denoted as Mn4. D1–E333 also participates in the coordination of $Mn_4$. The same carboxylic group(s) participate in the ligation of either manganese or iron. Interestingly, aspartic acid (D1–D170) also provides a ligand to a $Ca^{2+}$ cation and is also the bridge between these two cations (Umena et al. 2011). Therefore, we suggest the existence of a $Ca^{2+}$-cation effect on the interaction of Fe(II) with the HA site.

The blocking process of the HA site by iron cation(s) in PSII(-Mn) membranes commences with the weak binding of an Fe(II) to the HA Mn-binding site; the weakly bound Fe(II) cation is then oxidized by a light-induced $Y_Z^{\bullet+}$ radical (Semin et al. 2002). This is the first step of blocking process. The efficiency of Fe(II) oxidation at the HA site can be measured separately using the flash-probe fluorescence method. While only one Fe(III) cation blocks the HA site, the oxidation of 4–5 Fe(II) cations is required to complete the blocking process (Semin and Seibert 2004). This bound Fe(III) as mentioned above prevents the further interaction of exogenous Mn(II) cations with this site and hence the donation of electrons to $Y_Z^{\bullet+}$ via this site. This is the second step of the blocking process. Completion of both steps is termed the entire blocking process. The efficiency of blocking can also be estimated by measuring electron donation efficiency of via the HA site by Mn(II) cations after blocking. Taking this mechanism of blocking into account, we studied the effect of $Ca^{2+}$ cations on the donation of electrons by Fe(II) cations to $Y_Z^{\bullet+}$ during the light-dependent oxidation process and then on the entire blocking process of the HA sites by Fe(III) cations. Donation of electrons was monitored using flash-probe fluorescence (Ghirardi et al. 1996). The $F_{max}$ and $F_{fin}$ values were used to determine the efficiency of donation, using the equation, $[(F_{max} - F_{fin})/F_{max}]^{-Fe(II)} - [(F_{max} - F_{fin})/F_{max}]^{+Fe(II)}$ (Semin et al. 2002). Here, $F_{fin}$ is the final fluorescence yield detected after decay of the flash-induced $F_{max}$ and $F_{max}$ is the maximum fluorescence yield following actinic flash excitation. $Ca^{2+}$ inhibition of the flash-induced donation of electrons by Fe(II) cations (5 μM) to $Y_Z^{\bullet+}$ is shown in Fig. 1 (curve 1). The results show the inhibition of Fe(II) oxidation, which reaches a maximum level of 25% at rather high $Ca^{2+}$ concentration (about 25 mM, where the Ca/Fe ratio is equal to 5000).

The $Ca^{2+}$ concentration dependence on the entire blocking process [electron donation plus tight binding of the Fe(III)] is also shown in Fig. 1 (curve 2). Blocking of the HA site in the presence of different concentrations of $Ca^{2+}$ was carried out by incubating PSII(-Mn) membranes with Fe(II) for 3 min under weak light. The efficiency of blocking was estimated as the efficiency of donation after blocking compared to that before, measured as described above. The results demonstrate that $Ca^{2+}$ added together with Fe(II) to PSII(-Mn) samples before incubation decreased the efficiency of blocking. The maximal level of inhibition was observed in the same $Ca^{2+}$ concentration region as was the case for donation (curve 1), but the efficiency of inhibition was greater (about 40% compared to 25%). By comparing the results (inhibition by $Ca^{2+}$ of both Fe(II) oxidation and Fe(III) blocking), we note the following: (1) Since the efficiency of these two processes is different, this means that oxidation of Fe(II) cations at the HA site (first step of the blocking process, which can be measured in the absence of the second) is only the initial part of the blocking process. (2) The second step of the blocking process following Fe(II) oxidation is the strong binding of a newly generated Fe(III) cation with the Mn-binding site. The efficiency of the inhibition of the second step is about 15% (40%–25%). (3) The concentration dependence of Fe(II) oxidation (curve 1) and the entire blocking process by

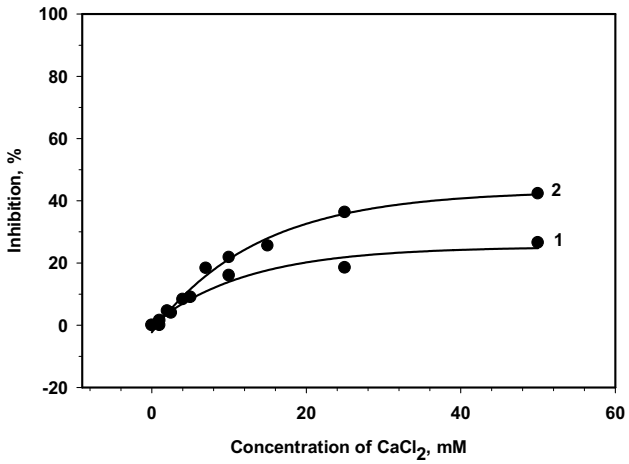


**Fig. 1** Effect of $Ca^{2+}$ concentration on the donation to (first step in the text) and blocking of (second step in the text) PSII(-Mn) membranes by iron as determined by the flash-probe fluorescence method. *1* $Ca^{2+}$ inhibition of flash-induced donation of electrons by exogenous Fe(II) cations (5 μM) in PSII(-Mn) membranes to $Y_Z^{\bullet+}$. *2* $Ca^{2+}$ inhibition of the entire blocking process (see text) associated with the HA site: PSII(-Mn) membranes (25 μg Chl $ml^{-1}$) were incubated in buffer A with $FeSO_4$ (5 μM) + $Ca^{2+}$ under room light (4 μE $m^{-2}$ $s^{-1}$) for 3 min. The samples were then pelleted and resuspended in buffer A (at 25 μg Chl $ml^{-1}$), and the flash-fluorescence decay profile was measured in the presence of 40 μM DCMU. The level of blocking in % was determined by estimating Fe(II) (10 μM) donation in blocked membranes, using the equation noted in the text, relative to the 100% control (donation in non-blocked PSII(-Mn) membranes). Data are average of three independent experiments

$Ca^{2+}$(curve 2) are similar, saturating at 25–50 mM $Ca^{2+}$. The same concentration dependence occurs in the case of the activation of oxygen evolution by $Ca^{2+}$ in PSII(-Ca) membranes (Tamura et al. 1989; Miyao-Tokutomi and Inoue 1992). These results suggest that the effect of Ca on the entire blocking process is the result of conformational changes induced by the interaction of the $Ca^{2+}$ ion with its specific binding site, which in turn affects the HA site.

In the above-described experiments, $Ca^{2+}$ was present in the sample during the blocking process. We also investigated the $Ca^{2+}$ effect when incubation occurred before and after blocking the PSII(-Mn) membranes (Table 1, rows 4, 5). $Ca^{2+}$ does not change the fluorescence decay curve very much, if the Ca ions were added after the PSII(-Mn) membranes were blocked (Fig. 2). $Ca^{2+}$ addition to blocked PSII(-Mn) membranes (Table 1, row 5) also had little effect on electron donation. Furthermore, the efficiency of Fe(II) oxidation did not change, if $Ca^{2+}$ was added before addition of Fe(II) (Table 1, row 4). In this case, membranes were incubated with $Ca^{2+}$ for 15 min to bind a $Ca^{2+}$ ion to the Ca-binding site, then unbound $Ca^{2+}$ was removed by centrifugation, and the membranes were washed with buffer A prior to incubating with Fe(II) to block the HA site. However, the absence of a tightly bound $Ca^{2+}$ ion to Ca-binding site in this experiment cannot be excluded.

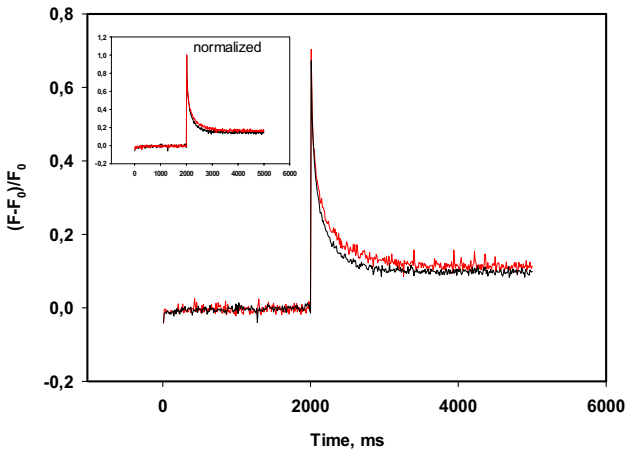


**Fig. 2** $Ca^{2+}$ effects on the charge recombination rate between $Q_A^-$ and $Y_Z^{\bullet+}$ in blocked PSII(-Mn) membranes as determined by flash-probe fluorescence. The concentration of the PSII(-Mn) membranes was 25 µg Chl $ml^{-1}$ in buffer A. Fluorescence decays were measured in the presence of 40 µM DCMU without (*black curve*) or in the presence of 50 mM $CaCl_2$ (*red curve*). Fluorescence was measured 2–3 min after $Ca^{2+}$ addition. No Fe(II) was present in this experiment. Each fluorescence kinetic trace is an average of three decays

**Table 1** Effect of calcium on blocking of the HA Mn-binding site by Fe cations

| Sample | Donation[a] by Fe(II) (%) | Half-time ($t_{1/2}$, ms) of fluorescence decay[b] |
|---|---|---|
| PSII(-Mn) | 100 ± 1[c] | 31 ± 1 |
| PSII(-Mn)[d] + 50 mM $Ca^{2+}$ | 73 ± 2 | 51 ± 1[e] |
| PSII(-Mn,+Fe)[f] | 8 ± 2 | 46 ± 2 |
| PSII(-Mn) membranes were incubated with 50 mM $Ca^{2+}$ | | |
| Before blocking[g] | 4 ± 1 | 50 ± 1 |
| After blocking[h] | 3 ± 0.5 | 42 ± 3 |

[a]Light-induced electron donation by Fe(II) cations (10 µM) in each case was calculated using the equation $[(F_{max}-F_{fin})/F_{max}]^{-Fe(II)}-[(F_{max}-F_{fin})/F_{max}]^{+Fe(II)}$ (Semin et al. 2002)

[b]Fluorescence decay represents charge recombination between $Q_A^-$ and $Y_Z^{\bullet+}$. The half-time is the time constant of the decay kinetics and reflects the rate of the recombination process

[c]100% control = 0.65 ± 0.01, no $Ca^{2+}$ added

[d]$Ca^{2+}$ was added to the PSII(-Mn) membranes. Then Fe(II) cations were added for measurement of donation. Fluorescence decay for $t_{1/2}$ determination was measured without Fe(II) in the presence of $Ca^{2+}$ cations

[e]There is a small difference between this value and the value for a similar sample presented in Fig. 3 ($t_{1/2} \approx 57$ ms). This difference can be explained by small differences in the respective preparations as well as deviations in the pHs of the buffers since the pH dependence of the $t_{1/2}$ values in PSII(-Mn) membranes changes rapidly in the pH region from 6.0 to 8.0 (Semin and Seibert 2004)

[f]Blocked PSII membranes: PSII(-Mn) membranes (25 µg Chl $ml^{-1}$) were incubated in buffer A (pH 6.5) containing 5 µM Fe(II) for 3 min under low light (5 µE $m^{-2}$ $s^{-1}$). No $Ca^{2+}$ was added

[g]PSII(-Mn) membranes were incubated with $Ca^{2+}$ for 15 min in dark, and then $Ca^{2+}$ was removed by centrifugation before blocking

[h]PSII(-Mn, + Fe) membranes were incubated with $Ca^{2+}$ in the dark for 30 min after blocking

Nevertheless, we do note that $Ca^{2+}$ ions significantly affect the rate of fluorescence decay, representing the charge recombination between $Q_A^-$ and $Y_Z^{\bullet+}$. The half-time ($t_{1/2}$) of fluorescence decay is a time constant that reflects the rate of the recombination process. It is equal to 31 ± 1 ms in control PSII(-Mn) membranes, but $Ca^{2+}$ addition decreases the recombination rate to 51 ± 1 ms (Table 1, rows 1 and 2). This is understandable since the Ca-binding site is close to Yz, and water molecule, W4 (a ligand to Ca), forms a hydrogen bond with $Y_Z$. Also, another water molecule, W3 bound to a Ca ion, is connected to $Y_Z$ via water molecule, W7 (Kawakami et al. 2011). The saturation of this effect is observed beginning at a $Ca^{2+}$ concentration of about 10 mM (Fig. 3). It should be noted that the $t_{1/2}$ for a $Ca^{2+}$ concentration of 50 mM is about 57 ms (the $Ca^{2+}$ saturation level in Fig. 3). There is some difference (about 10–12%) between this value and the value for a similar sample presented in Table 1 (51 ± 1 ms). Possible reasons for this difference are noted in a footnote of Table 1. Interestingly, blocking of the HA site with iron also increases the rate fluorescence decay (to 46 ± 2 ms) as in the case with $Ca^{2+}$ (Table 1, compare row 1 with rows 2 and 3). The HA site is also close to $Y_Z$ and $Mn_4$, the latter of which occupies the site in native PSII membranes. $Mn_4$ also interacts with $Y_Z$ via the hydrogen

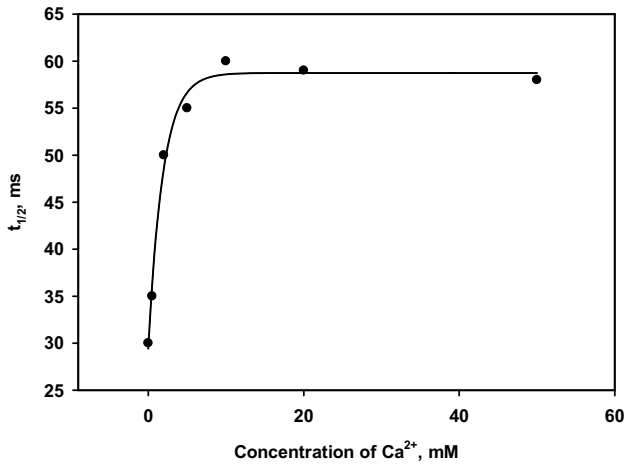


**Fig. 3** $Ca^{2+}$ effect on the rate of fluorescence decay in PSII(-Mn) membranes (25 µg Chl $ml^{-1}$ in buffer A). Flash-probe fluorescence kinetics were measured in the presence of 40 µM DCMU. No Fe(II) was present in this experiment. Data are average of three independent experiments

bond net, including water molecules W2 (ligand to $Mn_4$), W3 (ligand to $Ca^{2+}$), and W5–W7 (Kawakami et al. 2011). However, in the case of simultaneous application of both metal cations [Fe(II) and $Ca^{2+}$], the decrease in the recombination rate is not the sum of the two effects but corresponds only to effect of one cation. So, for example, addition of $Ca^{2+}$ to PSII(-Mn,+Fe) membranes does not significantly influence the recombination rate ($t_{1/2}=42\pm3$ ms vs. $46\pm2$ ms). We have found that the pH dependence of $t_{1/2}$ values in PSII(-Mn) membranes (Semin and Seibert 2004) changes rapidly in the pH region from 6.0 to 8.0.

## $Ca^{2+}$ effects on the substitution of Mn cations in the OEC with Fe cations

Incubation of PSII(-Ca) membranes with Fe(II) cations in the dark is accompanied by the substitution of one (at pH 5.7) or two (at pH 6.5) Mn ions with Fe cation(s) (Semin and Seibert 2016; Semin et al. 2018). Fe(II) cations chemically reduce available Mn cations in the Mn cluster; reduced Mn(II) cations are released from their binding site(s), and Fe(III) cation(s) formed by the oxidation of the Fe(II) cations occupy the vacant Mn site(s). Using this model of substitution (Semin and Seibert 2016; Semin et al. 2018), we investigated the effect of $Ca^{2+}$ cations on the Fe for Mn exchange process. Table 2 clearly shows that $Ca^{2+}$ ions prevent the substitution of 1Mn ion at pH 5.7 [the residual quantity of Mn after treatment with Fe(II) is 4Mn/reaction center (RC)] and also 1Mn ion at pH 6.5 [the residual quantity of Mn after treatment with Fe(II) is 3Mn/RC]. This effect is specific since it is observed not only for $Ca^{2+}$ cations but also for $Sr^{2+}$ cations (see Table 3). It is known that $Sr^{2+}$ is the only

**Table 2** Effect of $Ca^{2+}$ ions on the extraction of Mn cations from the OEC by Fe(II) at different pHs

| Sample | Mn/RC | |
|---|---|---|
| | pH 5.7 | pH 6.5 |
| PSII(-Ca) without Fe(II) treatment | 4.0 ± 0.2 | 4.0 ± 0.2 |
| PSII(-Ca) after incubation with Fe(II) | 2.9 ± 0.2 | 2.0 ± 0.1 |
| PSII(-Ca) after incubation with Fe(II) in the presence of 10 mM $Ca^{2+}$ | 3.9 ± 0.2 | 3.1 ± 0.2 |

Treatment with Fe(II): PSII(-Ca) samples (100 µg Chl $ml^{-1}$) were incubated with 20 µM $FeSO_4$

for 120 min in dark at 4 °C. After incubation, the membranes were pelleted, washed in buffer A, and then resuspended in buffer A for determination of the Mn contents

other metal cation besides $Ca^{2+}$ that can restore $O_2$-evolving activity in the Ca-depleted PSII membranes (to about 40% of the control $O_2$-evolution activity at saturating light intensity Ghanotakis et al. 1984a). According to Vrettos et al. (2001b), the ability of $Sr^{2+}$ to substitute for $Ca^{2+}$ in the OEC is the result of similarities in the p*K*a of the aqua ion bound to the cations and ionic radius of cations (see Table 3).

The effect of inhibition by $Ca^{2+}$ on the substitution of 1Mn cation in the OEC with Fe(II) is also supported by measurements of fluorescence induction kinetics (Fig. 4). The FIK of the native PSII preparations (Fig. 4, curve 1) increases from the minimum level of O to the P level (maximum) due to the reduction of $Q_A$ and $Q_B$ by electrons coming from the OEC (Lazar 1999). Extraction of a $Ca^{2+}$ cation from the OEC results in almost complete inhibition of oxygen release; however, the reduction of the exogenous

**Table 3** The ability of different metal cations to prevent the extraction of a Mn ion from the Mn cluster by Fe(II) cations

| Ion[a] | Content of Mn/RC[b] | pK of the aqua ion[c] | Radius (Å)[c] |
|---|---|---|---|
| $+La^{3+}$ | 1.8 ± 0.1 | 8.82 | 1.02 |
| $+Cd^{2+}$ | 1.8 ± 0.1 | 9.00 | 0.97 |
| $+Ni^{2+}$ | 1.7 ± 0.1 | 9.40 | 0.69 |
| $+Mg^{2+}$ | 2.0 ± 0.1 | 11.42 | 0.66 |
| $+Ca^{2+}$ | 3.1 ± 0.2 | 12.80 | 0.99 |
| $+Sr^{2+}$ | 3.1 ± 0.2 | 13.18 | 1.12 |

[a]Control contents of Mn/RC in the PSII(-Ca) membranes without treatment and after treatment of PSII(-Ca) membranes with only Fe(II) cations (without addition of any ions) are presented in Table 2

[b]Treatment with Fe(II): PSII(-Ca) samples (100 µg Chl $ml^{-1}$) were incubated with 20 µM $FeSO_4$ in the presence of 10 mM of the indicated metal cation for 120 min in dark at +4 °C in buffer A (pH 6.5). After incubation, the membranes were pelleted, washed in buffer A, and resuspended in buffer A for determination of the Mn content. See Table 2, row 2 for the control Mn/RC content for the experiment in row 5 above as measured in the absence of added $Ca^{2+}$

[c]Data from (Dean 1985)

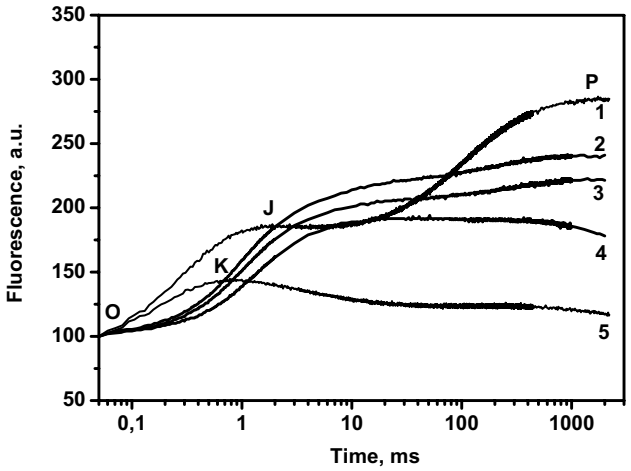


**Fig. 4** Fluorescence induction curves of chlorophyll *a* in different membrane preparations of PSII (25 μg Chl $ml^{-1}$) measured in buffer A at pH 6.5. *1* PSII [the rate of DCPIP reduction was 132 ± 5 μmol DCPIP mg $Chl^{-1}$ $h^{-1}$ (100%)]; *2* PSII(-Ca) membrane preparations (DCPIP reduction, 69 ± 3%); *3* PSII(3Mn,1Fe) sample prepared by incubation of PSII(-Ca) membranes (100 μg Chl $ml^{-1}$) with 20 μM Fe(II) and 10 mM $Ca^{2+}$ at pH 6.5 (DCPIP reduction, 22 ± 3%); *4* PSII (2Mn,2Fe) prepared at pH 6.5 (DCPIP reduction, 17 ± 2%); *5* PSII (-Mn) (DCPIP reduction, 5 ± 1%)

electron acceptor, DCPIP, is inhibited much less efficiently (the remaining activity is about 70% Semin et al. 2008). This effect was termed decoupling (Semin et al. 2008). The study of the mechanism behind this ("decoupling" effect, not related to the uncoupling of ATP) has shown that electron transport in the absence of oxygen release is due to incomplete oxidation of water, which only proceeds to $H_2O_2$ instead of $O_2$ (i.e., the oxidation of water to $H_2O_2$ ensures the generation of electrons in PSII(-Ca) preparations for donations to $Q_A$ and $Q_B$) (Semin et al. 2013). The presence of electron flow in the PSII(-Ca) samples is shown by the FIK of this sample (Fig. 4, curve 2), which is similar to the fluorescence kinetics of intact PSII membranes (Semin et al. 2008). Substitution of 2 or 1Mn ions with Fe ions inhibits electron transport (DCPIP reduction) but not completely. Note in Fig. 4 that the sample with 3Mn/RC is more active than the sample with 2Mn/RC (Semin and Seibert 2016; Semin et al. 2018). Electron-transport activity after total Mn extraction by Tris treatment is absent (Semin and Seibert 2016; Semin et al. 2018). We measured the FIK curve of PSII(2Mn,2Fe) samples in Fig. 4, curve 4. The maximum P ($F_{max}$) of this curve is significantly lower than that of curve 2 for PSII(-Ca) samples. Furthermore, if the sample contains 3Mn/1Fe (Table 2, row 3, pH 6.5), the fluorescence curve (Fig. 4, curve 3) has a larger $F_{max}$ than that seen in curve 4, but similar to FIK curve 2 in PSII(-Ca) membranes. These results show that the electron-transport activity of this sample is higher than the activity of the PSII(2Mn,2Fe) sample [i.e., during incubation with Fe(II) together with $Ca^{2+}$ at pH 6.5, the OEC in PSII(-Ca) membranes lose only 1Mn, not 2, supporting results presented in Table 2].

Other cations ($La^{3+}$, $Cd^{2+}$, $Ni^{2+}$, and $Mg^{2+}$) do not prevent the extraction of Mn cations in the OEC by Fe(II) (Table 3). It has been suggested that the value of the pK of the aqua metal cation is important for the ability of the cation to restore $O_2$-evolution function in PSII(-Ca) membranes (Vrettos et al. 2001b). However, according to Table 3, the atomic radius of the cation may also be a factor. Our results show that one Mn cation in the cluster is under rather effective $Ca^{2+}$ control. A bound Ca cation increases the resistance of this Mn cation to chemical reduction by exogenous reductants. In our previous work, we have shown that in the case of the substitution of 2Mn ions with Fe (at pH 6.5) (Semin and Seibert 2016), one of the extracted Mn is bound to the HA site (Mn4). The sensitivity of one of the Mn cations to $Ca^{2+}$ action at both pH 5.7 and 6.5 (Table 2) allows us to conclude that this Mn binds to the HA site since there is structural proximity of the Ca-binding site. Both sites (for Mn4 and $Ca^{2+}$) interact with each other via direct hydrogen bonds between water molecules, W2 (ligand to Mn4) and W3 (ligand to Ca), as well as with the hydrogen bond net, including the W5–W7 water molecules (Kawakami et al. 2011). Moreover, these two metal cations are mutually connected via the carboxylic group of D1–D170 and the oxygen bridge, O5, in native PSII preparations (Kawakami et al. 2011). However, it should be noted that such a tight interaction between Mn and $Ca^{2+}$ cations via hydrogen bonds and ligands can occur only in the intact PSII. In our work, we used mainly PSII(-Mn) and Ca-depleted PSII membranes. It can be assumed that in Mn-depleted and Ca-depleted membranes, these hydrogen bonds are broken. In this regard, we note that the Zouni group (Zhang et al. 2017) recently found that extraction of the Mn/Ca cluster by hydroxylamine from PSII crystals (prepared from native PSII cores) leaves the positions of all the coordinating residues and most of the nearby water molecules largely unaffected. However, recently Gisriel et al. (2020) using cryo-EM methods have shown that the configuration of ligands coordinating the $Mn_4CaO_5$ cluster in apo-PSII from *Synechocystis* sp. PCC 6803 differs from the ligand sphere configuration in the native PSII. These results were supported by data obtained by Zabret et al. (2020) and Tokano et al. (2020). Apparently, the absence of changes in the ligand positions (after extraction of the OEC cluster by hydroxylamine from crystals of PSII) may be due to stabilization of the structure by crystal packing forces (Gisriel et al. 2020; Zabret et al. 2020). Taking these data into account, we suggest that in PSII(-Mn) membranes, the $Ca^{2+}$ effect on Fe(II) oxidation/blocking is most likely due to competition of Fe and Ca cations for negatively charged amino acids, D1–D170 and D1–E333 associated with the Mn-binding HA site. In the case of PSII(-Ca) membranes, the situation is most likely different. Although

a $Ca^{2+}$ cation is extracted from the OEC, the Ca-binding site is still functional since it can bind a $Ca^{2+}$ cation, and this binding is accompanied by the restoration of $O_2$-evolution activity (Ghanotakis et al. 1984a). Therefore, $Ca^{2+}$ effects on the substitution of Mn by Fe can be explained by the interaction of a bound $Ca^{2+}$ cation with Mn ions through the OEC ligands and/or hydrogen bond net. Our results demonstrate that exogenous $Ca^{2+}$ prevents the extraction of 1Mn cation (by Fe[II]) from the OEC at both pH 5.7 and pH 6.5 (Table 2). Since extraction of Mn from the OEC results from the reduction of Mn cations in the structure and their subsequent release, we also conclude that the bound calcium ion probably changes the redox potential of the extractable Mn cation (Mn4), making it resistant to reduction.

**Acknowledgements** The work (MS) at the National Renewable Energy Laboratory (NREL) was carried out under US Department of Energy contract number DE-AC36-08-GO28308. MS also acknowledges the support of the NREL Emeritus Program.

## Compliance with ethical standards

**Conflict of interest** The authors declare that they have no conflict of interest.

## References

Ananyev GM, Dismukes GC (1996) High-resolution kinetic studies of the reassembly of the tetra-manganese cluster of photosynthetic water oxidation: proton equilibrium, cations, and electrostatics. Biochemistry 35:14608–14617. https://doi.org/10.1021/bi960894t

Armstrong JM (1964) The molar extinction coefficient of 2,6-dichlorophenolindophenol. Biochim Biophys Acta 86:194–197. https://doi.org/10.1016/0304-4165(64)90180-1

Dean JA (ed) (1985) Lange's handbook of chemistry. McGraw-Hill Book Co, New York

Ghanotakis DF, Babcock GT (1983) Hydroxylamine as an inhibitor between Z and P680 in photosystem II. FEBS Lett 153:231–234. https://doi.org/10.1016/0014-5793(83)80154-9

Ghanotakis DF, Babcock GT, Yocum CF (1984a) Calcium reconstitutes high rates of oxygen evolution in polypeptide depleted photosystem II preparations. FEBS Lett 167:127–130. https://doi.org/10.1016/0014-5793(84)80846-7

Ghanotakis DF, Topper JN, Yocum CF (1984b) Exogenous reductants reduce and destroy the Mn-complex in photosystem II membranes depleted of the 17 and 23 kDa polypeptides. Biochim Biophys Acta 767:524–531. https://doi.org/10.1016/0005-2728(84)90051-3

Ghanotakis DF, Babcock GT, Yocum CF (1984c) Structural and catalytic properties of the oxygen-evolving complex. Correlation of polypeptide and manganese release with the behavior of $Z^+$ in chloroplasts and a highly resolved preparation of the PSII complex. Biochim Biophys Acta 765:388–398. https://doi.org/10.1016/0005-2728(84)90180-4

Ghirardi ML, Lutton TM, Seibert M (1996) Interactions between diphenylcarbazide, zinc, cobalt, and manganese on the oxidizing side of photosystem II. Biochemistry 35:1820–1828. https://doi.org/10.1021/bi951657d

Gisriel CJ, Zhou K, Huang H-L, Debus RJ, Xiong Y, Brudvig GW (2020) Cryo-EM structure of monomeric photosystem II from *Synechocystis* sp. PCC 6803 lacking the water-oxidation complex. Joule 4(10):2131–2148. https://doi.org/10.1016/j.joule.2020.07.016

Kawakami K, Umena Y, Kamiya N, Shen J-R (2011) Structure of the catalytic, inorganic core of oxygen-evolving photosystem II at 1.9 Å resolution. J Photochem Photobiol B 104:9–18. https://doi.org/10.1016/j.jphotobiol.2011.03.017

Kern J, Chatterjee R, Young ID, Fuller FD, Lassalle L, Ibrahim M, Gul S, Fransson T, Brewster AS, Alonso-Mori R, Hussein R, Zhang M, Douthit L, de Lichtenberg C, Cheah MH, Shevela D, Wersig J, Seuffert I, Sokaras D, Pastor E, Weninger C, Kroll T, Sierra RG, Aller P, Butryn A, Orville AM, Liang M, Batyuk A, Koglin JE, Carbajo S, Boutet S, Moriarty NW, Holton JM, Dobbek H, Adams PD, Bergmann U, Sauter NK, Zouni A, Messinger J, Yano J, Yachandra VK (2018) Structures of the intermediates of Kok's photosynthetic water oxidation clock. Nature 563:421–425. https://doi.org/10.1038/s41586-018-0681-2

Kim CJ, Debus RJ (2017) Evidence from FTIR difference spectroscopy that a substrate $H_2O$ molecule for $O_2$ formation in photosystem II is provided by the Ca ion of the catalytic $Mn_4CaO_5$ cluster. Biochemistry 56:2558–2570. https://doi.org/10.1021/acs.biochem.6b01278

Lazar D (1999) Chlorophyll a fluorescence induction. Biochim Biophys Acta 1412:1–28. https://doi.org/10.1016/S0005-2728(99)00047-X

Miyao-Tokutomi M, Inoue Y (1992) Improvement by benzoquinones of the quantum yield of photoactivation of photosynthetic oxygen evolution: direct evidence for the two-quantum mechanism. Biochemistry 31:526–532. https://doi.org/10.1021/bi00117a032

Najafpour MM, Renger G, Hołyńska M, Moghaddam AN, Aro EM, Carpentier R, Nishihara H, Eaton-Rye JJ, Shen J-R, Allakhverdiev SI (2016) Manganese compounds as water-oxidizing catalysts: from the natural water-oxidizing complex to nanosized manganese oxide structures. Chem Rev 116:2886–2936. https://doi.org/10.1021/acs.chemrev.5b00340

Nixon PJ, Diner BA (1992) Aspartate 170 of the photosystem II reaction center polypeptide D1 is involved in the assembly of the oxygen-evolving manganese cluster. Biochemistry 31:942–948. https://doi.org/10.1021/bi00118a041

Ono T, Inoue Y (1990) Abnormal redox reactions in photosynthetic $O_2$-evolving centers in NaCl/EDTA-washed PS II A dark-stable EPR multiline signal and an unknown positive charge accumulator. Biochim Biophys Acta 1020:269–277. https://doi.org/10.1016/0005-2728(90)90157-Y

Porra RJ, Thompson WA, Kriedemann PE (1989) Determination of accurate extinction coefficients and simultaneous-equations for assaying chlorophyll-A and chlorophyll-B extracted with 4 different solvents: verification of the concentration of chlorophyll standards by atomic-absorption spectroscopy. Biochim Biophys Acta 975:384–394. https://doi.org/10.1016/S0005-2728(89)80347-0

Preston C, Seibert M (1991) The carboxyl modifier 1-ethyl-3-[3-(dimethylamino)propyl] carbodiimide (EDC) inhibits half of the high-affinity manganese-binding site in photosystem II membrane fragments. Biochemistry 30:9615–9624. https://doi.org/10.1021/bi00104a008

Semin BK, Ghirardi ML, Seibert M (2002) Blocking of electron donation by Mn(II) to $Y_Z^{\bullet}$ following incubation of Mn-depleted photosystem II membranes with Fe(II) in the light. Biochemistry 41:5854–5864. https://doi.org/10.1021/bi0200054

Semin BK, Seibert M (2004) Iron bound to the high-affinity Mn-binding site of the oxygen-evolving complex shifts the pK of a component controlling electron transport via Y(Z). Biochemistry 43:6772–6782. https://doi.org/10.1021/bi036047p

Semin BK, Seibert M (2006) A carboxylic residue at the high-affinity, Mn-binding site participates in the binding of iron cations that

block the site. Biochim Biophys Acta 1757:189–197. https://doi.org/10.1016/j.bbabio.2006.02.001

Semin BK, Davletshina LN, Ivanov II, Rubin AB, Seibert M (2008) Uncoupling of processes of molecular synthesis and electron transport in the $Ca^{2+}$-depleted PSII membranes. Photosynth Res 98:235–249. https://doi.org/10.1007/s11120-008-9347-5

Semin BK, Seibert M (2009) A simple colorimetric determination of the manganese content in photosynthetic membranes. Photosynth Res 100:45–48. https://doi.org/10.1007/s11120-009-9421-7

Semin BK, Davletshina LN, Timofeev KN, Ivanov II, Rubin AB, Seibert M (2013) Production of reactive oxygen species in decoupled, $Ca^{2+}$-depleted PSII and their use in assigning a function to chloride on both sides of PSII. Photosynth Res 117:385–399. https://doi.org/10.1007/s11120-013-9870-x

Semin BK, Seibert M (2016) Substituting Fe for two of the four Mn ions in photosystem II: effects on water-oxidation. J Bioenerg Biomembr 48:227–240. https://doi.org/10.1007/s10863-016-9651-2

Semin BK, Davletshina LN, Seibert M, Rubin AB (2018) Creation of a 3Mn/1Fe cluster in the oxygen-evolving complex of photosystem II and investigation of its functional activity. J Photochem Photobiol B 178:192–200. https://doi.org/10.1016/j.jphotobiol.2017.11.016

Serrat FB (1998) 3,3′,5,5′-Tetramethylbenzidine for the colorimetric determination of manganese in water. Mikrochim Acta 129:77–80. https://doi.org/10.1007/BF01246852

Suga M, Akita F, Hirata K, Ueno G, Murakami H, Nakajima Y, Shimizu T, Yamashita K, Yamamoto M, Ago H, Shen J-R (2015) Native structure of photosystem II at 1.95 Å resolution viewed by femtosecond X-ray pulses. Nature 517:99–103. https://doi.org/10.1038/nature13991

Suga M, Akita F, Sugahara M, Kubo M, Nakajima Y, Nakane T, Yamashita K, Umena Y, Nakabayashi M, Yamane T, Nakano T, Suzuki M, Masuda T, Inoue S, Kimura T, Nomura T, Yonekura S, Yu L-J, Sakamoto T, Motomura T, Chen J-H, Kato Y, Noguchi T, Tono K, Joti Y, Kameshima T, Hatsui T, Nango E, Tanaka R, Naitow H, Matsuura Y, Yamashita A, Yamamoto M, Nureki O, Yabashi M, Ishikawa T, Iwata S, Shen J-R (2017) Light-induced structural changes and the site of O=O bond formation in PSII caught by XFEL. Nature 543:131–135. https://doi.org/10.1038/nature21400

Tamura N, Cheniae GM (1987) Photoactivation of the water-oxidizing complex in photosystem II membranes depleted of Mn and extrinsic proteins. I. Biochemical and kinetic characterization. Biochim Biophys Acta 890:179–194. https://doi.org/10.1016/0005-2728(87)90019-3

Tamura N, Inoue Y, Cheniae GM (1989) Photoactivation of the water-oxidizing complex in photosystem II membranes depleted of Mn, Ca and extrinsic proteins: II. Studies on the functions of $Ca^{2+}$. Biochim Biophys Acta 976:173–181. https://doi.org/10.1016/S0005-2728(89)80227-0

Tokano T, Kato Y, Sugiyama S, Uchihashi T, Noguchi T (2020) Structural dynamics of a protein domain relevant to the water-oxidizing complex in photosystem II as visualized by high-speed atomic force microscopy. J Phys Chem B 124(28):5847–5857. https://doi.org/10.1021/acs.jpcb.0c03892

Tsui EY, Agapie T (2013) Reduction potentials of heterometallic manganese–oxido cubane complexes modulated by redox-inactive metals. Proc Natl Acad Sci USA 110:10084–10088. https://doi.org/10.1073/pnas.1302677110

Umena Y, Kawakami K, Shen J-R, Kamiya N (2011) Crystal structure of oxygen-evolving photosystem II at a resolution of 1.9 Å. Nature 473:55–65. https://doi.org/10.1038/nature09913

Vrettos JS, Limburg J, Brudvig GW (2001a) Mechanism of photosynthetic water oxidation: combining biophysical studies of photosystem II with inorganic model chemistry. Biochim Biophys Acta 1503:229–245. https://doi.org/10.1016/S0005-2728(00)00214-0

Vrettos JS, Stone DA, Brudvig GW (2001b) Quantifying the ion selectivity of the $Ca^{2+}$ site in photosystem II. Evidence for direct involvement of $Ca^{2+}$ in $O_2$ formation. Biochemistry 40:7937–7945. https://doi.org/10.1021/bi010679z

Xu Q, Bricker TM (1992) Structural organization of proteins on the oxidizing side of photosystem I. Two molecules of the 33-kDa manganese-stabilizing proteins per reaction center. J Biol Chem 267:25816–25821

Zabret J, Bohn S, Schuller SK, Arnolds O, Möller M, Meier-Credo J, Liauw P, Chan A, Tajkhorshid E, Langer JD, Stoll R, Krieger-Liszkay A, Engel BD, Rudack T, Schuller JM, Nowaczyk MM (2020) How to build a water-splitting machine: structural insights into photosystem II assembly. bioRxiv. https://doi.org/10.1101/2020.09.14.294884

Zhang M, Bommer M, Chatterjee R, Hussein R, Yano J, Dau H, Kern J, Dobbek H, Zouni A (2017) Structural insights into the light-driven auto-assembly process of the water-oxidizing $Mn_4CaO_5$-cluster in photosystem II. eLife 6:e26933. https://doi.org/10.7554/eLife.26933